

## Neoclassical Poloidal Rotation Studies in High Temperature Plasmas

W.M. Solomon,<sup>1</sup> K.H. Burrell,<sup>2</sup> R. Andre,<sup>1</sup> L.R. Baylor,<sup>3</sup> R.E. Bell,<sup>1</sup> R. Budny,<sup>1</sup> P. Gohil,<sup>2</sup>  
R.J. Groebner,<sup>2</sup> G.J. Kramer,<sup>1</sup> R. Nazikian,<sup>1</sup> G. Rewoldt,<sup>1</sup> E.J. Synakowski,<sup>1</sup> W. Wang,<sup>1</sup>  
and M.C. Zarnstorff<sup>1</sup>

<sup>1</sup>Princeton Plasma Physics Laboratory, Princeton, New Jersey, USA

<sup>2</sup>General Atomics, San Diego, California, USA

<sup>3</sup>Oak Ridge National Laboratory, Oak Ridge, Tennessee, USA

The determination of poloidal rotation from charge exchange measurements is made difficult due to various atomic physics effects. The energy dependence of the charge exchange cross-section necessitates that large corrections be applied to the measured line of sight velocities. Uncertainties in the effective cross-section caused by excited beam neutrals further complicate the problem. We perform the analysis using an integrated approach, simultaneously fitting all the charge exchange rotation measurements. Even after considering the necessary corrections, the measurements still indicate discrepancy with the neoclassical theory of poloidal rotation.

### I Introduction

Rotation plays an important role in the suppression of turbulence and the formation of internal transport barriers through  $E \times B$  shear. Despite the importance of rotation to high performance operation, momentum confinement remains a poorly understood topic in fusion plasmas. This is in part related to the difficulty of performing accurate poloidal rotation measurements. Recent improvements in measurement and analysis capabilities of the DIII-D charge exchange recombination (CER) system [1,2] now make it feasible to test the neoclassical theory of poloidal rotation.

### II. Complications in Interpreting Rotation from Charge Exchange Measurements

The determination of plasma rotation from charge exchange measurements is complicated by various atomic physics effects. The fundamental problem results from the energy dependence of the charge exchange cross section [3]. The corrections that are required to account for these effects can be substantial. In the case of poloidal rotation, corrections of order one are generally necessary, while the toroidal rotation often needs to be corrected by more than 100 km/s on DIII-D. The magnitude of these corrections is sensitive to the details of the cross-section, and increases with increasing ion temperature.

Originally, it was thought that there would be no effect due to the energy-dependent cross-section on views perpendicular to the neutral beam. However, owing to the finite lifetime of the excited charge exchange state, coupled with the gyro-motion of the ions, the correction caused by the distortion of the lineshape due to the energy-dependent cross-section can precess into the vertical viewing direction, and hence affect poloidal rotation measurements [4]. In DIII-D, where the neoclassically predicted poloidal rotation is generally less than 1–2 km/s, it is clearly important to accurately handle the atomic physics corrections for the vertical views if one is to attempt a significant comparison with theory.

The line-of-sight (LOS) velocities of all the CER chords are simultaneously processed to give the actual toroidal and poloidal rotation. By making use of vertical chords close to the magnetic axis, it is possible to separate out the gyro-orbit correction from the actual poloidal rotation [5]. Such chords measure predominantly atomic physics corrections only, since there is effectively no plasma poloidal velocity near the axis.

### III. Validation of Cross-Section Model

The details of the cross-section model can have significant impact on the inferred rotation. This is particularly the case for the toroidal rotation analysis. Figure 1 shows the charge exchange cross-section, interpolated for relevant plasma conditions from the ADAS database for the C-VI ( $n=8 \rightarrow 7$ ) transition [6]. The presence of less than 1% of beam neutrals in an excited  $n=2$  state can significantly alter the effective cross-section [Fig. 1(c)], since the  $n=2$  cross-section [Fig. 1(b)] is two orders of magnitude larger than the simple  $n=1$  capture cross-section [Fig. 1(a)] at low energies. For reference, the positions of the full, half and third energy components of a typical 80 keV  $D_2$  beam (in this example shifted to lower interaction energies by rapid plasma rotation  $\sim 500$  km/s) is overplotted. The plot shows the cross-sections calculated at two radial locations ( $\rho \sim 0$  [black] and  $\rho \sim 0.5$  [red]). There is notable difference between the two effective cross-sections at low energies, largely owing to the different calculated contributions of  $n=2$  (0.3% vs 0.2%). At the half and third beam energies, the slope of the cross-section actually changes sign, and thus the amount of correction is reduced by as much as 40% near the magnetic axis compared with using the  $n=1$  cross-section alone.

Since the results are quite sensitive to the details of the cross-section model, we need a method to ensure that our calculated cross-sections are consistent with the data. We have investigated two techniques to test the validity of the cross-section model. The first utilizes a nominally radial chord, passing through the magnetic axis. Such a chord measures essentially *only* cross-section correction and provides quite a strong test of the cross-section model. Figure 2 shows the measured LOS velocity for the radial chord during a high ion temperature ( $T_i \sim 15$  keV) QH-mode discharge on DIII-D [7]. Also shown is the reconstructed LOS velocity based on the simple  $n=1$  capture cross-section (blue), and the calculated effective cross-section (green). It is clear that the  $n=1$  cross-section overestimates the magnitude of the LOS velocity, but the calculated effective cross-section appears to almost equally underestimate the measurement. One can argue that the distortion to the cross-section is not as severe as calculated (possibly

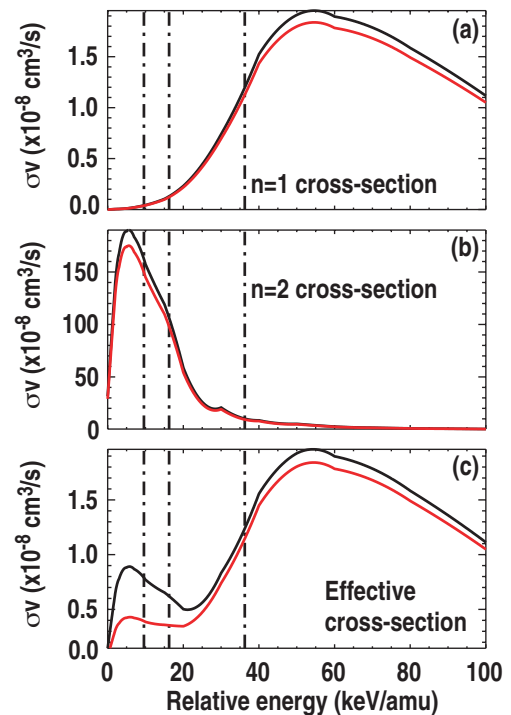


Fig. 1. Distortion of effective charge exchange cross-section in the presence of excited beam neutrals at 2 radial locations: on-axis (black) and mid-radius (red) for a typical set of plasma parameters. (a)  $n=1$  capture cross-section, (b)  $n=2$  cross-section, (c) effective cross-section taking into account relative  $n=2$  contributions.

meaning the actual population of  $n=2$  is less than expected). In red, an intermediate cross-section with a reduced  $n=2$  population is used, which correctly reproduces the measurement.

A second check is made by exploiting a geometry dependence of the cross-section correction. The correction points in a direction predominantly along the neutral beam vector [5]. Hence, the amount of correction that a view chord receives depends on its angle with respect to the beam. On the DIII-D CER system, there exist interspersed views from two nearby ports. One can demand that the corrected velocities from the two different views lie on the same smooth curve. The LOS velocities for three chords are plotted in Fig. 3, along with their expected values based on an interpolation from the neighboring views at the other port. The left column shows the measured LOS velocities, clearly illustrating that the measurements from the two separate views are not consistent and need to be corrected. The corrected measurements on the right (using the intermediate cross-section determined from the radial chord) show excellent agreement. Although this is not an extremely sensitive test of the cross-section, it does verify that the cross-section necessary to describe the radial chord is consistent with the tangential measurements.

#### IV Results

The global fit of the LOS measurements for all tangential and vertical chords is shown in Fig. 4. The plasma is an ELM-suppressed H-mode making use of the I-coil [8]. The plasma conditions on axis are  $T_i \sim 15$  keV,  $T_e \sim 4$  keV,  $n_e \sim 5 \times 10^{18} \text{ m}^{-3}$ , with 10 MW of co-injected neutral beam power. One can see that the fit using the splines described in Ref. [5] accurately reproduces all the measurements. The breakdown of the contributions to the LOS velocity for a vertical chord at  $\rho \sim 0.25$  is shown in Fig. 5. The magenta shows the contribution to the measurement made by the poloidal rotation. Accounting for the toroidal

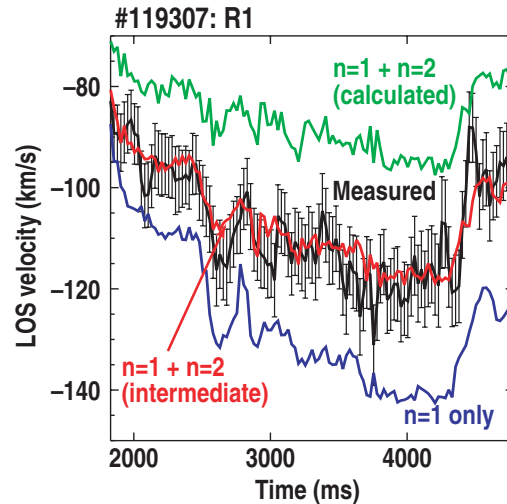


Fig. 2. Measured LOS velocity for a radial chord (black), with reconstructed value based on  $n=1$  cross-section only (green), effective cross-section using calculated  $n=2$  fractions (blue), and intermediate cross-section (red).

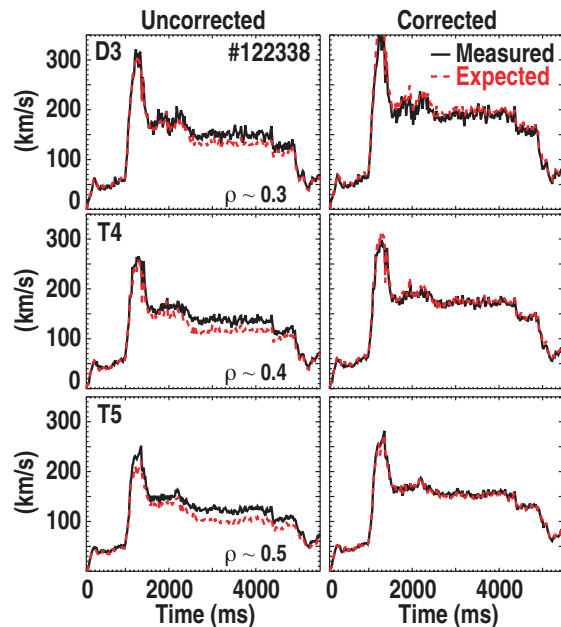


Fig. 3. Measured (black) LOS velocities of three tangential chords [ $\rho \sim (0.3, 0.4, 0.5)$ ] and the expected values (red) based on interpolation from chords with different viewing geometry. On the left, the uncorrected LOS velocities show that the measurement sets do not lie on the same smooth curve, but after correction on the right, the agreement is good.

rotation pickup due to the non-ideal geometry of the chord, we would measure what is shown in blue, assuming there was no energy-dependence of the cross-section. Allowing for the energy-dependent cross-section, we move to the green curve and, including the gyro correction, we arrive at the red curve, in good agreement with the measurement. Thus, the actual poloidal rotation only makes up a small fraction of the total vertical chords measurement.

The poloidal rotation profile, averaged over the ELM-free period from 3000-4000 ms, is shown in Fig. 6. The dashed curves surrounding the solid plot represent the standard deviation of the time-resolved profiles over the time window. Also shown is the neoclassically predicted poloidal rotation for carbon, obtained from the code NCLASS [9] using the front-end code FORCEBAL. Even accounting for all the details of the cross-section, the two profiles are not in agreement, and for most of the plasma radius the theory predicts rotation in the opposite direction than what is observed.

This work was supported by the US DOE under DE-AC02-76CH03073, DE-FC02-04ER54698, and DE-AC05-00OR22725.

- [1] K.H. Burrell, *et al.*, Rev. Sci. Instrum. **72**, 1028 (2001).
- [2] K.H. Burrell, *et al.*, Rev. Sci. Instrum. **75**, 3455 (2004).
- [3] M. von Hellermann, *et al.*, Plasma Phys. Control. Fusion **37**, 71 (1995).
- [4] R.E. Bell and E.J. Synakowski, AIP Conf. Proc. **547**, 39 (2000).
- [5] W.M. Solomon, *et al.*, Rev. Sci. Instrum. **75**, 3481 (2004).
- [6] H.P. Summers, JET Joint Undertaking Report, JET-IR(94)-06, <http://patiala.phys.strath.ac.uk/adas>.
- [7] K.H. Burrell, *et al.*, Phys Plasmas **8**, 2153 (2001).
- [8] T.E. Evans, *et al.*, Phys. Rev. Lett. **92**, 235003 (2004).
- [9] W.A. Houlberg, *et al.*, Phys. Plasmas **4**, 3230 (1997).

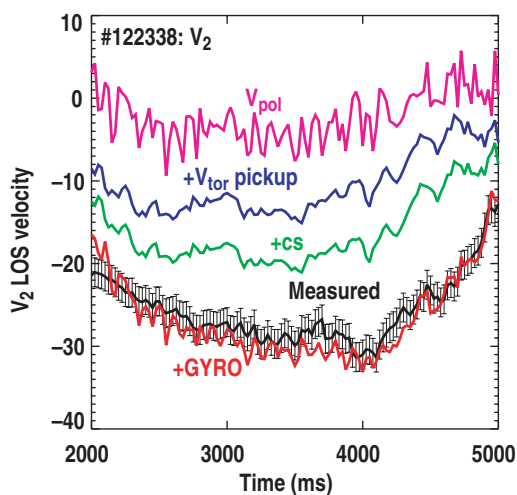


Fig. 5. Measured LOS velocity (black) of V2 chord ( $\rho \sim 0.25$ ), showing the contribution as additional physics comprising this measurement is included: Poloidal rotation (magenta), toroidal rotation pickup (blue), cross-section correction (green), and gyro-correction (red).

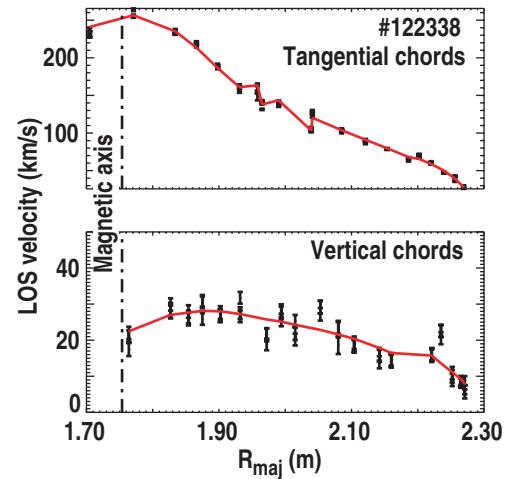


Fig. 4. Measured LOS velocities for (a) tangential and (b) vertical viewing CER chords. The red points are the measured values with error bars, while the black squares are the re-projected LOS velocities after solving for the toroidal and poloidal rotation. The jaggedness in the tangential profile arises because the chords view the plasma from two distinct ports with different toroidal angles.

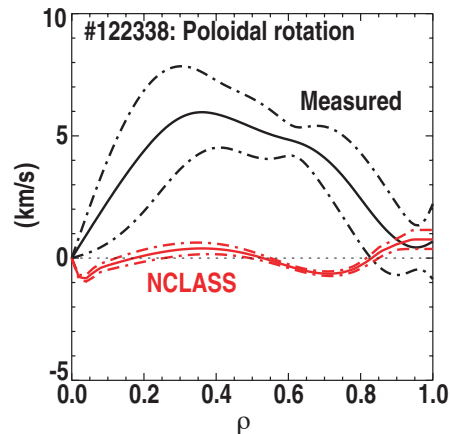


Fig. 6. Corrected poloidal rotation profile [black], averaged over an ELM-free period between 3000–4000 ms, compared with the neoclassical prediction from NCLASS averaged over the same period. The dashed bands represent the error estimate, obtained from the standard deviation of the time resolved profiles during the time window.